APPLIED AND ENVIRONMENTAL MICROBIOLOGY, Aug. 2005, p. 4487–4496 Vol. 71, No. 8
0099-2240/05/$08.00+0 doi:10.1128/AEM.71.8.4487–4496.2005

Isolation and Characterization of a Genetically Tractable Photoautotrophic Fe(II)-Oxidizing Bacterium, *Rhodopseudomonas palustris* Strain TIE-1

Yongqin Jiao, Andreas Kappler,† Laura R. Croal, and Dianne K. Newman*

Division of Geological and Planetary Sciences, California Institute of Technology, Pasadena, California

Received 10 December 2004/Accepted 11 March 2005

We report the isolation and characterization of a phototrophic ferrous iron [Fe(II)]-oxidizing bacterium named TIE-1 that differs from other Fe(II)-oxidizing phototrophs in that it is genetically tractable. Under anaerobic conditions, TIE-1 grows photoautotrophically with Fe(II), H_2, or thiosulfate as the electron donor and photoheterotrophically with a variety of organic carbon sources. TIE-1 also grows chemoheterotrophically in the dark. This isolate appears to be a new strain of the purple nonsulfur bacterial species *Rhodopseudomonas palustris*, based on physiological and phylogenetic analysis. Fe(II) oxidation is optimal at pH 6.5 to 6.9. The mineral products of Fe(II) oxidation are pH dependent: below pH 7.0 goethite (α-FeOOH) forms, and above pH 7.2 magnetite (Fe_3O_4) forms. TIE-1 forms colonies on agar plates and is sensitive to a variety of antibiotics. A hyperactive mariner transposon is capable of random insertion into the chromosome with a transposition frequency of $\sim 10^{-5}$. To identify components involved in phototrophic Fe(II) oxidation, mutants of TIE-1 were generated by transposon mutagenesis and screened for defects in Fe(II) oxidation in a cell suspension assay. Among approximately 12,000 mutants screened, 6 were identified that are specifically impaired in Fe(II) oxidation. Five of these mutants have independent disruptions in a gene that is predicted to encode an integral membrane protein that appears to be part of an ABC transport system; the sixth mutant has an insertion in a gene that is a homolog of CobS, an enzyme involved in cobalamin (vitamin B_{12}) biosynthesis.

Phototrophic Fe(II)-oxidizing bacteria were first reported over a decade ago (20, 57), but very little is known about how these bacteria oxidize Fe(II) at the molecular level. In part, this is due to the lack of a genetic system in any of these isolates. Accordingly, we set out to isolate a new Fe(II)-oxidizing species that would be amenable to genetic analysis. We were motivated to understand the process of phototrophic Fe(II) oxidation in detail because it likely represents one of the most ancient forms of photosynthesis and organisms with this metabolism may have catalyzed the deposition of banded iron formations (BIFs), an ancient class of iron-containing sediments (20, 36, 57). To test the hypothesis that Fe(II)-oxidizing phototrophs played a role in BIF deposition at discrete intervals in earth history, we must be able to evaluate putative molecular biosignatures that are preserved in ancient rocks. These biosignatures generally fall into two classes: organic and inorganic. At present, there are no unique organic biomarkers associated with this physiology, nor are there clear inorganic biosignatures, although stable Fe isotopes may hold promise in this regard (14). Given this, elucidation of the molecular components of the phototrophic Fe(II) oxidation pathway is necessary both to constrain our interpretation of the Fe-isotopic fractionation produced by these bacteria and to identify biomolecules specific to Fe(II) oxidation that may be preserved over geologic time (14).

To date, the phototrophic Fe(II)-oxidizing bacteria that have been isolated are phylogenetically diverse and include members of the purple sulfur (*Thiodictyon* sp. strain F4), purple nonsulfur (*Rhodobacter ferrooxidans* strain SW2 and *Rhodovulum* sp. strains N1 and N2), and green sulfur (*Chlorobium ferrooxidans* KoFox) bacteria (14, 20, 27, 53). In addition to the Fe(II)-oxidizing phototrophs, Fe(II) oxidation is also catalyzed by nitrate-dependent Fe(II)-oxidizing bacteria (4, 37) and acidophilic or neutrophilic Fe(II)-oxidizing aerobic microorganisms (19, 22, 52, 55). Most of what is known about the molecular mechanisms of Fe(II) oxidation derives from biochemical studies of the acidophilic Fe(II)-oxidizing aerobe *Acidithiobacillus ferrooxidans* (13). Proteins thought to be involved in the transfer of electrons from Fe(II) to O_2 include the blue copper protein rusticyanin (11, 12), a high-redox-potential Fe-S protein (23), an outer membrane porin (46), several types of cytochromes (1, 42, 56, 60), and one or more cytochrome oxidases (29). The exact role of each of these carriers in the electron transport pathway of Fe(II) oxidation, however, is uncertain and controversial. In particular, there is debate on where Fe(II) oxidation takes place in the cell (2, 5, 58), although there is general agreement that the Fe(II) oxidase is located external to the cytoplasmic membrane.

Here, we describe the isolation and characterization of a genetically tractable Fe(II)-oxidizing phototroph that is closely related to the type strain of *Rhodopseudomonas palustris*. As a first step in the identification of the molecular components of the phototrophic Fe(II) oxidation pathway, we performed a genetic screen to identify genes involved in Fe(II) oxidation. The potential functions of these genes in the process of phototrophic Fe(II) oxidation are discussed.

* Corresponding author. Mailing address: California Institute of Technology, Division of Geological and Planetary Sciences, Mail Stop 100-23, Pasadena, CA 91125. Phone: (626) 395-6790. Fax: (626) 683-0621. E-mail: dkn@gps.caltech.edu.

† Present address: Center for Applied Geoscience, University of Tübingen, Tübingen, Germany.

TABLE 1. Bacterial strains and plasmids used in this study

Strain or plasmid	Genotype or markers, characteristics, and uses	Source or reference
E. coli strains		
β2155	Donor for bacterial conjugation; *ThrB1004 pro thi strA hsdS lacZΔM15* (F′ *lacZΔM15 lacI*^{q} *trajD36 proA*$^+$ *proB*$^+$) Δ*dapA*::*erm* (Erm^r) *pir*::RP4 [::*kan* (Km^r) from SM10]	17
WM3064	Donor strain for conjugation; *thrB1*004 *pro thi rpsL hsdS lacZ*ΔM15 RP4-1360 Δ(*araBAD*)*567* Δ*dapA*1341::[*erm pir*(wt)]	W. Metcalf, Univ. of Illinois, Urbana
UQ950	DH5α λ (pir) host for cloning; F$^-$ Δ(*argF-lac*)*169* ϕ80d*lacZ58*(ΔM15) *glnV44*(AS) *rfbD1 gyrA96*(NalR) *recA1 endA1 spoT1 thi-1 hsdR17 deoR* λ *pir*$^+$	D. Lies, Caltech
R. palustris strain		
CGA009	Wild type (ATCC BAA-98)	34
Plasmids		
pSC189	Transposon delivery plasmid; NCBI accession no. AY115560	10
pRK415	10.5-kb incP-1 (pK2) Tc^r lacZ	32
pT198	T198 PCR fragment, including the promoter region, cloned into the Xba I site of pRK415	This study
pT498	T498 PCR fragment, including the promoter region, cloned into the Xba I site of pRK415	This study

MATERIALS AND METHODS

Bacterial strains and plasmids. Bacterial strains and plasmids used in this study are listed in Table 1.

Media and culture conditions. Basal medium for phototrophic Fe(II)-oxidizing bacteria was prepared as described by Ehrenreich and Widdel (20). Medium containing dissolved Fe(II) but no Fe(II) precipitates [called filtered Fe(II) medium] was prepared by adding $FeCl_2$ (to a final concentration of 10 mM) and subsequent filtration of the precipitated Fe(II) minerals, leaving ~4 mM Fe(II) in solution (for details, see reference 14). Fe(II)-containing medium refers to filtered Fe(II) medium unless specified otherwise. For phototrophic growth with Fe(II) as the electron donor, cultures were incubated at 30°C in Fe(II)-containing medium with an N_2-CO_2 (80:20) headspace of ~20 cm distance from a 40-W incandescent light bulb. For phototrophic growth with H_2 as the electron donor, H_2 was supplemented in the headspace (H_2-CO_2, 80:20). For aerobic growth, TIE-1 was grown in YP medium that contained 0.3% yeast extract and 0.3% Bacto Peptone (Difco). *Escherichia coli* strains were cultured in Luria-Bertani broth at 37°C (44). *E. coli* β2155 and WM3064 were supplemented with DAP (diaminopimelic acid, 300 μM final concentration). Kanamycin and tetracycline were used at 200 and 50 μg/ml for TIE-1 and 50 and 15 μg/ml for *E. coli*, respectively.

Isolation. Cultures of phototrophic Fe(II)-oxidizing bacteria were enriched by inoculating medium supplemented with 10 mM $FeCl_2$ (without filtration) with samples taken from an iron-rich mat from School Street Marsh in Woods Hole, Mass. Enrichments were incubated at room temperature in the light. After a few days, rusty patches developed on the inner surface of the bottles. Cultures containing rusty patches were transferred successively to Fe(II)-containing medium. After three transfers, the enrichments were subjected to an anaerobic agar dilution series, where 6 ml of prewarmed medium supplemented with $FeCl_2$ and 1 ml of bacterial culture were mixed with 3 ml of 3% (wt/vol) molten agar in a test tube under a constant N_2 stream. Sequential dilutions were made by transferring 1 ml of bacteria-agar mix from one tube to the next until a series of 10 tubes were completed. The tubes were incubated in the light at room temperature (22°C). After 2 weeks, ovoid-shaped red colonies consisting of cells and rusty particles developed. Colonies were picked and subcultured in the filtered Fe(II)-containing medium. To select specifically for Fe(II)-oxidizing bacteria that could grow aerobically on agar plates, colonies formed in the agar dilution tubes were streaked to YP agar plates and incubated aerobically at 30°C in the dark. Agar dilution series were repeated three times to obtain pure cultures; the purity was checked by phase-contrast microscopy.

Analytical techniques. Fe(II) oxidation was monitored by measuring the consumption of Fe(II) over time. Fe(II) was quantified by the ferrozine assay (51). Cell mass was quantified by protein content determined by the method of Bradford (6), using reagents obtained from Bio-Rad (Richmond, CA). The cell mass versus protein ratio was determined with 200 ml of cell culture grown with 10 mM acetate phototrophically; cell mass was dried completely at 70°C. For protein measurement and microscopic cell counts of Fe(II)-grown cultures, the Fe(III) precipitates in 1 ml of culture were dissolved by addition of 800 μl of oxalate solution (28 g/liter of ammonium oxalate and 15 g/liter of oxalic acid in 1 liter ultrapure H_2O) plus 100 μl of ferrous iron ethylenediammonium sulfate (100 mM) as described by Suter et al. (54). Protein was precipitated by trichloroacetic acid (0.5 M), collected by centrifugation, and dissolved in NaOH (0.1 N) as described by Ehrenreich and Widdel (20). Cells were counted by epifluorescence microscopy after fixing with glutaraldehyde (2.5%) and staining with diamidino-2-phenylindole. The mineral products of Fe(II) oxidation were identified by X-ray diffraction (XRD) analysis as described by Kappler and Newman (31). Sample preparation and analysis by scanning electron microscopy (SEM), energy-dispersive spectroscopy (EDS), and transmission electron microscopy (TEM) were done as described by Kappler and Newman (31). MINEQL+ (Environmental Research Software) was used to calculate the Fe(II) speciation of the medium at different pH values given the total soluble Fe(II) concentration measured prior to inoculation. We assumed a closed system, and the model solution had basal component concentrations equal to the growth medium. We did not account for the small decrease of phosphate concentration by the precipitation of vivianite [$Fe_3(PO_4)_2 \cdot 8H_2O$] in our model, as the amount of phosphate removed from solution was less than 4% [estimated by assuming that the decrease in soluble Fe(II) measured at the highest pH tested, 7.5, was due to the precipitation of vivianite and calculating the corresponding amount of phosphate that would have been removed from solution]. The total Fe(II) concentration was set to the experimentally measured total dissolved Fe(II) concentration at different pH values, and no solid was removed. The ionic strength of the solution was not considered, and the temperature was set at 25°C.

Determination of physiological and phototrophic characteristics. To test for growth with different carbon sources, sterile stock solutions of various carbon sources (acetate, lactate, succinate, pyruvate, malate, fumarate, benzoate, formate, and glucose) were added to the basal medium at a final concentration of 10 mM. Sulfide, sulfite, and thiosulfate were tested as electron donors at 5 mM. Elemental sulfur (1 g/liter) was added from an autoclaved suspension, and growth was checked visually for pinkish turbidity. Growth of non-precipitate-containing cultures was monitored by increase of optical density at 600 nm. To determine the pH dependence of Fe(II) oxidation, the pH of the filtered Fe(II)-containing medium (initial pH, 6.8) was adjusted to between 5.5 and 7.5 with 1 M HCl or 1 M Na_2CO_3. The headspace of the cultures for this experiment was initially flushed with H_2-CO_2 (80:20) to stimulate bacterial growth, and end point measurements of Fe(II) concentration and protein content were taken after 5 days when Fe(II) oxidation had not proceeded to completion. Whole-cell absorption spectra were recorded in 40% (wt/vol) sucrose using a multidetection microtiter plate reader (Synergy HT; Bio-Tek, Winooski, VT). Carotenoids were extracted from phototrophically grown TIE-1 and *R. palustris* CGA009 cells. Cells from 15 ml of cultures grown with acetate as the electron donor were harvested by centrifugation (10 min; 7,800 × *g*). For pigment extraction, 5 ml of a mixture of acetone and ethanol (1:1) was added, and all of the following procedures were done under extremely dim light to protect the pigments from

phototransformations. The suspension was sonicated for 2 min and incubated in the dark at 30°C for 1 h. The pigments were transferred to hexane by adding 3 ml of hexane and 0.5 ml of H_2O followed by vigorous mixing. The upper phase was collected and replaced several times until it stayed clear. The combined hexane fractions were concentrated ~10-fold under a stream of N_2 and stored at −20°C before further analysis. The extracted pigments were separated using a normal-phase thin-layer chromatography (TLC) system with silica as adsorbent (Kieselgel 60; Merck, Darmstadt, Germany) and a mixture of petrol ether and acetone (4:1) as the mobile phase. Absorbance spectra of the crude extracts were recorded in a quartz 96-well microtiter plate and identified by comparison to extracts from the closely related reference strain *R. palustris* CGA009 (7).

16S rRNA sequence determination. Cells grown in YP medium for 2 days were harvested by centrifugation. Genomic DNA was extracted using the DNeasy kit (QIAGEN). 16S rRNA was amplified using primers 8F (5′-AGAGTTTGATC CTGGCTCAG-3′) and 1492R (5′-GGTTACCTTGTTACGATCC-3′). The PCR product was eluted in water after purification using a QIAquick PCR purification kit (QIAGEN). DNA was sequenced by the DNA Sequencing Core Facility at the Beckman Institute at Caltech using primers 8F and 1492R, with 2× coverage. Sequence alignment was performed on the National Center for Biotechnology Information (NCBI) website (http://www.ncbi.nlm.nih.gov/BLAST/). Distance and maximum likelihood phylogenetic trees were constructed using the ARB software package (40).

Antibiotic sensitivity. Sensitivity of strain TIE-1 to antibiotics (chloramphenicol, tetracycline, kanamycin, gentamicin, and ampicillin) was determined by growth tests on YP agar medium containing the antibiotics at various concentrations. A 100-μl aliquot of a cell suspension (~10^8 cells/ml) was spread on the agar plates with antibiotics, and the number of colonies formed was counted after aerobic incubation at 30°C in the dark for 5 days. The MIC was defined as the minimal antibiotic concentration at which no colonies formed on the plate during the allotted incubation time.

Genetic screen. To generate a library of transposon mutants to screen for Fe(II) oxidation defects, the plasmid pSC189, carrying the kanamycin-resistant hyperactive mariner transposon (10), was moved via conjugation from the donor strain *E. coli* β2155 to TIE-1. A deletion of the *dapA* gene of *E. coli* β2155 renders it unable to grow without the exogenous addition of DAP to the growth medium (17). Thus, TIE-1 exconjugants with transposon insertions can be selected on YP agar plates containing kanamycin (200 μg/ml) but no DAP. Transposon-containing TIE-1 exconjugants were picked to 96-well microtiter plates containing YP plus kanamycin and incubated aerobically at 30°C overnight with shaking. To test the transposon-containing isolates for Fe(II) oxidation activity in a cell suspension assay, 20 μl of the YP culture was transferred to a 96-well microtiter plate containing 200 μl phototrophic basal medium without Fe(II). These plates were incubated anaerobically in the light under an atmosphere of N_2-CO_2-H_2 (80:15:5) in an anaerobic glove box. After 3 days of incubation, the plates were centrifuged and the supernatant was removed. Under anaerobic conditions, cell pellets were resuspended in a buffer (50 mM HEPES, 20 mM NaCl, 20 mM $NaHCO_3$; pH 7) mixed with 200 to 300 μM of $FeCl_2$. After a 5-hour incubation in the light, 100 μl of ferrozine solution (1 g of ferrozine plus 500 g of ammonia acetate in 1 liter of double-distilled H_2O) was added into each well, and the optical density at 570 nm was recorded to determine the concentration of the remaining Fe(II) (51). Putative mutants were identified in instances where the total Fe(II) removed from the system was less than ~50% relative to the wild type. At least three independent checks were performed for each mutant.

Southern blotting. To verify that the mariner transposon inserted in a random fashion, we performed Southern blotting on 10 randomly selected mutants from different mating events. SmaI- and SphI-digested genomic DNA from the mutants was separated on a 1% agarose gel and transferred to nylon membrane using a positive pressure blotting apparatus (Stratagene, CA) according to the manufacturer's instructions. Probe DNA was prepared from a gel-purified MluI restriction fragment of pSC189 that contained an internal part of the mariner transposon including the kanamycin resistance gene. Approximately 25 ng of probe DNA was labeled with 50 μCi of [α-^{32}P]dCTP using Ready-To-Go labeling beads (Amersham Pharmacia Biotech). Prior to hybridization, unincorporated radioactive nucleotides were removed from the reaction mixture by centrifugation through Sephadex columns (ProbeQuant G-50 Microspin columns; Amersham Pharmacia Biotech) according to the manufacturer's instructions. Nylon membranes were hybridized overnight at 65°C. Hybridized membranes were washed three times for 5 min each in 2× SSC buffer (20× SSC is 175.3 g/liter NaCl plus 88.2 g/liter of trisodium citrate) plus 0.1% sodium dodecyl sulfate at room temperature and then twice for 15 min each with 0.1× SSC plus 0.1% sodium dodecyl sulfate at 65°C. The membrane was exposed to X-ray film at −80°C for 48 h prior to development.

Cloning of mariner-containing fragments. To identify the DNA sequence flanking the transposon in the mutants, genomic DNA was digested with restriction enzyme SacII followed by ligation at a DNA concentration (2 to 3 μg/ml) that favored intramolecular ligation (49). Ligated DNA was washed and concentrated using a DNA purification kit (QIAGEN) and transformed into *E. coli* UQ950 cells. Plasmid DNA was extracted from overnight cultures of kanamycin-resistant clones. The sites of transposon insertions of these mutants were determined by sequencing with primers Mar3 (5′-CTTCTTGACGAGTTCTTCTGA GC-3′) and Mar4 (5′-TAGGGTTGAGTGTTGTTCCAGTT-3′), which anneal near the ends of the mariner transposon in opposite directions. Sequence analysis and homology searches were performed by using the BLAST and the ORF Finder utilities that are available on the NCBI website (http://www.ncbi.nlm.nih.gov/BLAST/). Protein analysis, including subcellular localization analysis and motif finding, was done using TargetP and MotifScan on the ExPAsy proteomics server (http://us.expasy.org/).

Complementation. Plasmids pT198 and pT498 were constructed to complement the genetic defects in mutants 76H3 and A2, respectively. Primers were designed based on the corresponding gene sequences in *R. palustris* CGA009 that were analogous to the disrupted genes in the mutants. For mutant 76H3, a 1.4-kb gene fragment was amplified through PCR from wild-type TIE-1 with primers T198L (5′-GGCTCTAGATCAACCAGAAACCAGCTTCC-3′) and T198R (5′-GGCTCTAGATGTGAGCCACTCTGTCATCC-3′). For mutant A2, a 1.3-kb gene fragment was generated with primers T498L (5′-GGCTCTAGACAATTG CGACAGCTTACGAC-3′) and T498R (5′-GGCTCTAGAAGAACCGCCTTC TTGGTCT-3′). The purified PCR products were digested and ligated to the XbaI cloning site of the broad-host-range plasmid pRK415 vector to generate the vectors pT198 and pT498 for complementation. pT198 and pT498 were introduced into *E. coli* UQ950 by transformation. Transformants with the inserts were isolated through a blue/white screen on Luria-Bertani plates with tetracycline (15 μg/ml). The plasmids pT198 and pT498 were purified from *E. coli* UQ950, transformed by heat shock into the Δ*dapA* donor strain *E. coli* WM3064, and moved via conjugation into the mutant TIE-1 strains. TIE-1 exconjugants containing vectors pT198 and pT498 were selected on YP agar plates supplemented with 75 μg/ml of tetracycline. Colonies were picked and grown in YP liquid medium with tetracycline (75 μg/ml). YP cultures were washed and subcultured in the basal medium plus tetracycline (75 μg/ml) with H_2 as the electron donor. Cells were then collected by centrifugation and tested for complementation of Fe(II) oxidation activity by the cell suspension assay as described above.

Nucleotide sequence accession number. The 1,396-bp 16S rRNA sequence of TIE-1 was obtained and deposited in the GenBank database under the accession number AY751758.

RESULTS

Isolation. Phototrophic Fe(II)-oxidizing bacteria were enriched from samples taken from an iron-rich mat from School Street Marsh in Woods Hole, MA. The pH ranged from 6 to 7 at this site. Rusty orange-brown crusts formed on the inner surface of the enrichment bottles incubated in the light but not in the dark, suggesting the presence of phototrophic Fe(II)-oxidizing bacteria. After several transfers in liquid medium and purification in an agar dilution series, several isolates that looked microscopically identical were obtained. One isolate named TIE-1 was chosen for all further experiments. In the agar-shake tube, TIE-1 develops ovoid-shaped purple colonies containing orange-brown particles resembling iron rust. Phototrophically grown cells are motile and dumbbell shaped, with a length of 1 to 4 μm (Fig. 1A). The heterogenous cell morphology suggests that cells divide asymmetrically by budding, as is the case for closely related species (35). Electron microscopy revealed that phototrophically grown cells contained lamellar intracytoplasmic membranes (Fig. 1B). TIE-1 formed colorless colonies with purple centers on YP agar plates aerobically in the dark (Fig. 1C). TIE-1 is colorless in liquid medium under aerobic conditions and purple when grown phototrophically.

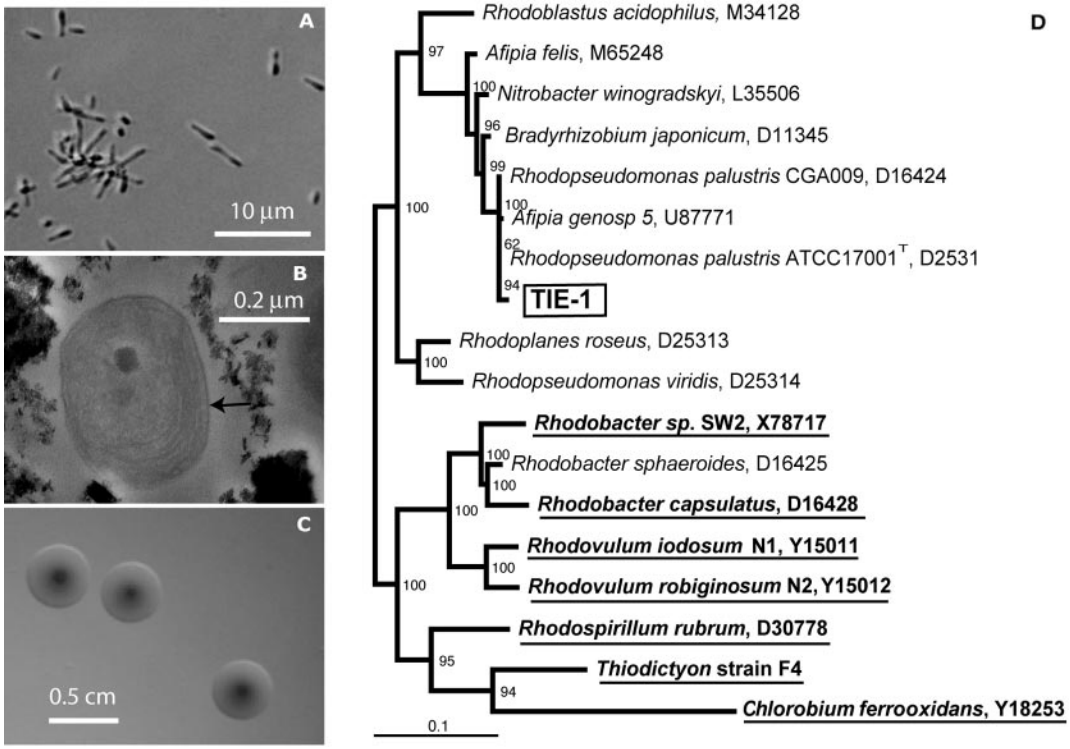

FIG. 1. (A) Phase-contrast micrographs showing the cell morphology of TIE-1 grown phototrophically with acetate as the electron donor. (B) Lamellar intracytoplasmic membranes (arrow) of a cell from a 1-week-old culture grown with Fe(II) as the electron donor. Fe(III) precipitates formed outside the cell. (C) Colony morphology on a YP agar plate incubated aerobically in the dark for 5 days. (D) 16S rRNA-based tree showing phylogenetic relationships between TIE-1 and related organisms. Bootstrap values are given at branch points. Anaerobic phototrophs able to oxidize Fe(II) are in boldface and underlined. TIE-1 (boxed) is separated significantly from the other known purple nonsulfur Fe(II)-oxidizing phototrophs, such as *Rhodobacter* sp. strain SW2 and *Rhodovulum* sp. strains N1 and N2.

Phylogeny. The 16S rRNA sequence was compared with the sequences from representative species of its close relatives along with the phototrophic Fe(II)-oxidizing bacteria that have been isolated so far (Fig. 1D). The 16S rRNA sequence of TIE-1 shares an identity of 98.9% and 99% to that of *Rhodopseudomonas palustris* ATCC 17001^T and strain CGA009, respectively, belonging to the α-subdivision of the *Proteobacteria*, affiliated closely with the nitrogen-fixing phototrophic rhizobia. TIE-1 clusters differently from the other known purple nonsulfur Fe(II)-oxidizing phototrophs, such as *Rhodobacter* sp. strain SW2 and *Rhodovulum* sp. strains N1 and N2.

Phototrophic oxidation of Fe(II). TIE-1 is able to grow photoautotrophically with Fe(II) as the electron donor under anaerobic conditions (Fig. 2). The increase in cell number is concomitant with the increase of protein content and the progress of Fe(II) oxidation throughout the incubation. No Fe(II) oxidation occurs for the duration of the incubation in abiotic controls, and bacterial growth and Fe(II) oxidation are light dependent (data not shown). Based on the experimentally determined ratio of protein to cell mass of 47%, there is 2.52 mg of protein, i.e., 5.36 mg of biomass produced per mmol of Fe(II) oxidized. This represents ~72% of the theoretical cell yield of 7.5 mg/mmol of Fe(II), based on the stoichiometry of CO_2 reduction coupled to Fe(II) oxidation according to the following equation: $4\ Fe^{2+} + HCO_3^- + 10\ H_2O = <CH_2O> + 7\ H^+ + 4\ Fe(OH)_3$. This number is comparable to what has been measured for a *Rhodomicrobium*-like isolate, which has 4.5 mg biomass produced per mmole of Fe(II) oxidized (57).

The final product of Fe(II) oxidation accumulates exclusively outside the cell in the form of Fe(III) precipitates. The

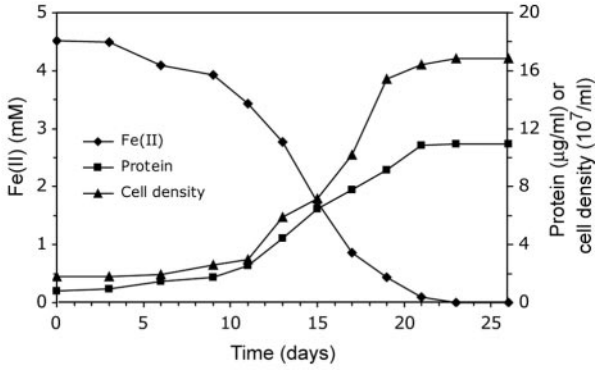

FIG. 2. Phototrophic growth of strain TIE-1 with Fe(II) as the electron donor. Shown are the Fe(II) concentration (◆), protein content (■), and cell density (▲). Data are representative of three independent cultures. The increase in cell number is consistent with the increase of protein content and the progress of Fe(II) oxidation throughout the incubation. No Fe(II) oxidation occurs for the duration of the incubation in the abiotic control, and bacterial growth and Fe(II) oxidation are light dependent (data not shown). Approximately 5.36 mg of biomass is produced per mmole of Fe(II) oxidized.

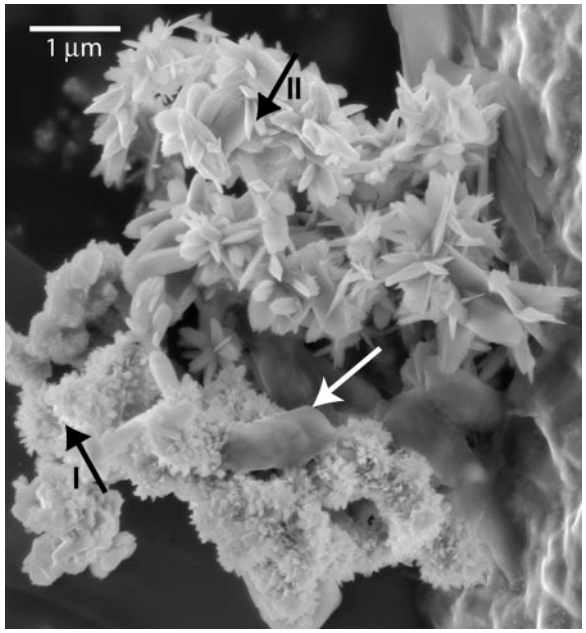

FIG. 3. Scanning electron micrograph of ferric iron precipitates produced by TIE-1, showing the presence of two types of Fe(III) minerals, including nanospherical (black arrow I) and needle-like (black arrow II) structures in a 2-week-old culture. The relative proportion of each morphological type varies with the age of the culture (see text). The white arrow indicates a TIE-1 cell.

spherical aggregates resembling poorly crystalline Fe(III) (hydr)oxides appear the most in the youngest cultures (1 week), and the more crystalline needle-like structures resembling goethite appear only in the older cultures (≥3 weeks). Figure 3 shows that the Fe(III) precipitates are of two morphologies in a 3-week-old Fe(II)-grown culture. One comprises small spherical aggregates of ~1 μm in size, and the other has a needle-like shape. TEM and XRD analyses suggest that the change of mineral morphology with time reflects mineral transformation, consistent with previous findings for minerals in cultures of *Rhodobacter* sp. strain SW2 (31). This type of mineral transformation is suggested to result from the adsorption of Fe(II) onto ferric (hydr)oxide, promoting its transformation to the thermodynamically more stable goethite (61). Elemental analysis of both types of precipitates using EDS gives signals only for iron and oxygen, with the atomic ratio (O/Fe) of 1.4 ± 0.1.

Physiological and biochemical characterizations. Similar to other *R. palustris* strains, TIE-1 was able to grow aerobically in the dark with a doubling time of ~3 h in YP medium (Fig. 4A). TIE-1 could also grow photoautotrophically with H_2 as the electron donor (Fig. 4B). Among sulfur compounds, TIE-1 uses thiosulfate, but not sulfide, elemental sulfur, or sulfite as an electron donor to support photosynthetic growth. Phototrophic growth of TIE-1 can be supported by a number of organic substrates, including acetate (Fig. 4C), lactate, succinate, pyruvate, malate, fumarate, and benzoate, but not formate or glucose (data not shown). We also tested Fe(III) reduction by TIE-1 and found that TIE-1 was not able to reduce Fe(III) citrate with acetate as the electron donor in the dark (data not shown). Fe(II) oxidation by TIE-1 is stimulated by the presence of H_2. In an atmosphere with 80% H_2, about 80% of the total Fe(II) in the system is oxidized within 5 days (data not shown), whereas the same amount of oxidation takes about 2 weeks when Fe(II) is the sole electron donor (Fig. 2). The cell density of a culture grown on H_2 (~10^9 cells/ml) is about 10 times as much as that when Fe(II) is the electron donor (Fig. 2 and Fig. 4B). Thermodynamically this makes sense, because the redox potential ($\Delta E_0'$) of the $2H^+/H_2$ redox couple (−0.41 V) (41) is significantly lower than that of the $Fe(OH)_3/Fe^{2+}$ redox couple (−0.11 V), calculated by setting $[Fe^{2+}]$ to 1 mM and assuming equilibrium constants given by Morel and Hering (47). H_2, therefore, is expected to be the preferred electron donor, providing more free energy to support bacterial growth. Cells grown on H_2 alone can immediately oxidize Fe(II), i.e., H_2 does not reduce the rate of Fe(II) oxidation (data not shown). Together, these results suggest that the stimulation of Fe(II) oxidation in the presence of H_2 is due to the stimulation of bacterial growth by H_2.

pH dependence of Fe(II) oxidation. To determine the optimal pH of Fe(II) oxidation by TIE-1, cells from Fe(II)-grown cultures were inoculated into Fe(II)-containing medium with H_2 in the headspace and the pH of the medium was adjusted to values spanning 5.5 to 7.5. Bacterial growth and dissolved Fe(II) were measured after a 5-day incubation. The pH was measured at the end of the experiment, and in each case was within 0.2 units of the initial pH. Appreciable Fe(II) oxidation occurred over the entire pH range tested; nevertheless, under these conditions the highest rate of Fe(II) oxidation occurred

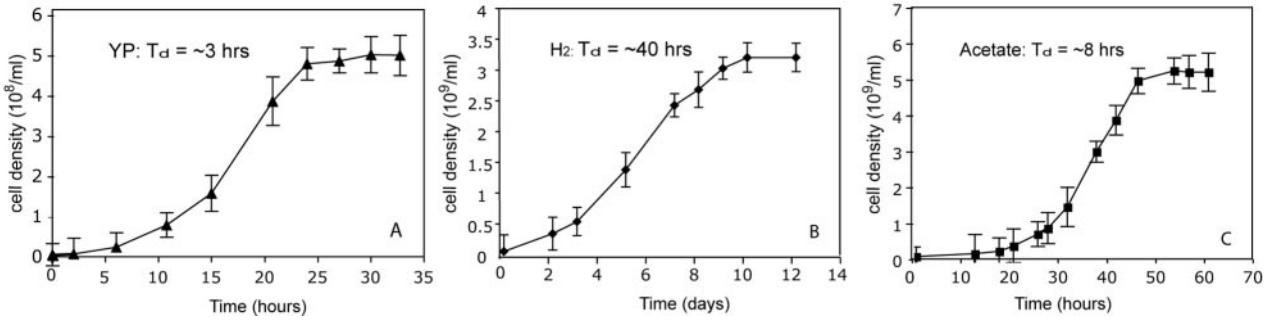

FIG. 4. Growth of TIE-1 chemoheterotrophically in YP medium aerobically in the dark (A), photoautotrophically with H_2 as the electron donor (B), and photoheterotrophically with acetate as the electron donor (C). Doubling time (T_d) was calculated for each growth condition from the slope of the curve over the exponential growth phase.

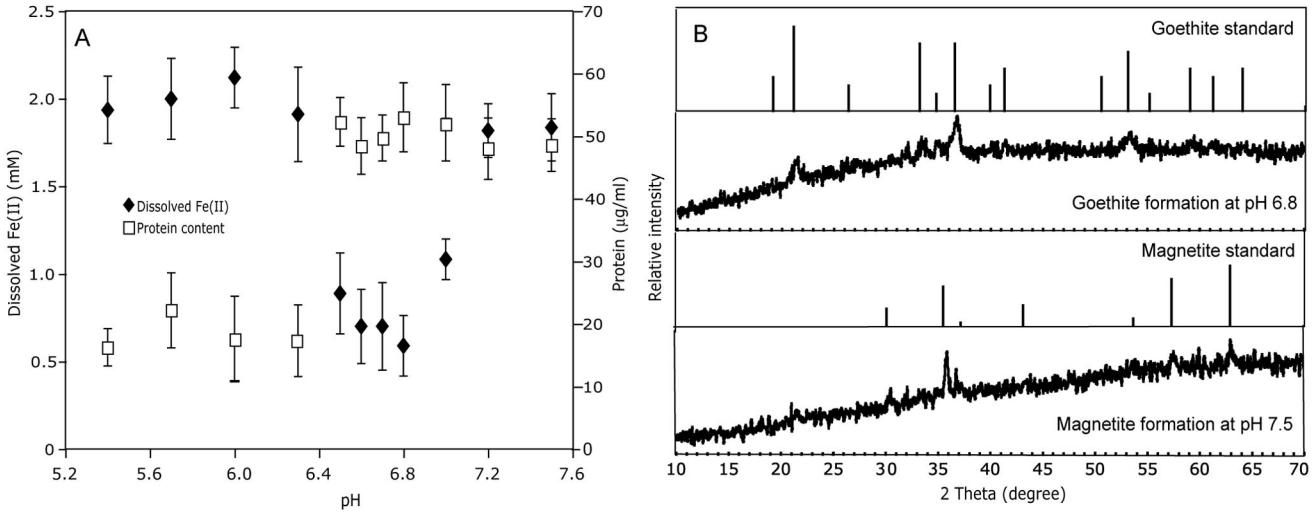

FIG. 5. (A) pH dependence of phototrophic Fe(II) oxidation in the presence of H_2: dissolved Fe(II) concentration in the supernatant at the end of the experiment (◆) and protein content after the incubation (□). The optimal pH for Fe(II) oxidation occurs from 6.5 to 6.9. The total amount of Fe(II) oxidized decreases significantly at pH higher than 7.0, although the amount of bacterial growth represented by the protein content remains constant compared to that at pH 6.8. (B) X-ray diffractograms of the product of Fe(II) oxidation by TIE-1 shows goethite and magnetite formation at media pHs of 6.8 and 7.5, respectively. For comparison, reference diffractograms of goethite and magnetite mineral standards are included.

between pH 6.5 and 6.9 (Fig. 5A), similar to the pH range measured for other phototrophic Fe(II)-oxidizing bacteria (20, 28). In contrast, the amount of bacterial growth (represented by the protein content) was maximal and not appreciably different within the pH range 6.5 to 7.5. This suggests that Fe(II) oxidation did not significantly contribute to cell growth in these experiments (i.e., cells were growing on H_2). We also observed that the mineral product of Fe(II) oxidation was pH dependent, with poorly crystalline ferric (hydr)oxide and goethite dominating at lower pH and magnetite at pH of $>7.2 \pm 0.2$ (Fig. 3 and 5B). The same pH trend in iron mineralogy was observed for cultures grown on Fe(II) alone (data not shown).

Because the total amount of dissolved Fe(II) remained in excess of 1.5 mM at a pH of ≥6.9, it seems unlikely that the amount of Fe(II) oxidation measured over this time period was limited by soluble Fe(II). However, the possibility exists that changes in concentration of a minor species of Fe(II) might have controlled the rate of Fe(II) oxidation. Considering this, we used MINEQL+ to calculate the equilibrium concentrations of soluble Fe(II) species over this pH range in the context of the composition of our medium. As pH increases from 6.5 to 7.5, MINEQL+ predicts that Fe^{2+} is the major Fe(II) species and only decreases by 0.4 mM over this pH range. Three minor Fe(II) species, including $Fe(OH)_3^-$, $Fe(OH)_{2(aq)}$, and $Fe(OH)^+$, increase in concentration 1,000-, 80-, and 10-fold, respectively. In the Discussion section, we consider how changes in these species' behaviors with increasing pH might affect the overall Fe(II) oxidation rate.

Pigment characterization. The absorption spectrum of whole cells of TIE-1 grown with acetate as the electron donor shows three major peaks at 590, 805, and 871 nm, similar to that of *R. palustris* CGA009, indicating the presence of bacteriochlorophyll *a*. The absorption spectrum obtained from TIE-1 grown with Fe(II) as the electron donor is similar and shows approximately the same peaks of absorbance as cells grown on acetate, except that the peak at 871 nm is wider for the Fe(II)-grown culture (Fig. 6A). The absorption spectra of carotenoid extracts (Fig. 6B) and thin-layer chromatography separations (data not shown) obtained from TIE-1 and CGA009 grown on acetate also look identical. The absorption

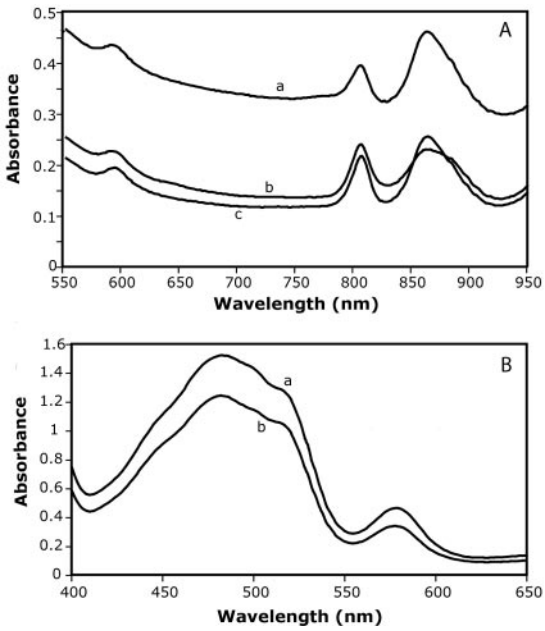

FIG. 6. Pigment analysis. (A) Absorption spectra of cell suspensions of strain TIE-1 grown with acetate (a) and Fe(II) (b) as the electron donor and of strain CGA009 grown with acetate as the electron donor (c) under phototrophic conditions. All curves look similar and show major absorption peaks at 590, 805, and 871 nm, indicating the presence of bacteriochlorophyll *a*. (B) Absorption spectra of carotenoid extraction from strain TIE-1 (a) and strain CGA009 (b) grown with acetate as the electron donor, showing major peaks that overlapped intensively between 400 and 600 nm, indicating the presence of the normal spirilloxanthin series.

spectra of carotenoid extracts show major peaks overlapping between 400 and 600 nm, suggesting the presence of carotenoids commonly present in *R. palustris*, including spheroidene (450, 482, and 514 nm), okenone (521 nm), lycopene, and rhodopin (463, 490, and 524 nm) (43).

Characterization of antibiotic sensitivity. Growth of $\sim 10^7$ cells on YP solid or liquid medium is inhibited completely by chloramphenicol (300 μg/ml), tetracycline (75 μg/ml), kanamycin (100 μg/ml), gentamicin (300 μg/ml), and ampicillin (50 μg/ml). These results indicate that it should be possible to select for the acquisition of these antibiotic resistance markers, which will facilitate genetic manipulation.

Transposon mutagenesis and mutant characterization. We used transposon mutagenesis to identify genes involved in phototrophic Fe(II) oxidation in strain TIE-1. The frequency of transposon insertion obtained for TIE-1 is $\sim 10^{-5}$ with the mariner transposon. Southern blot analysis of 10 randomly selected isolates derived from independent transposition events indicated that the transposon integrates as a single event in random locations (data not shown).

We performed a limited screen of ~12,000 transposon insertion mutants for defects in phototrophic Fe(II) oxidation using a cell suspension assay. Based on the assumptions that strain TIE-1 has the same number of genes as strain CGA009 and that the transposition is purely random, this screen is ~88% saturated assuming a Poisson distribution (26). Fourteen mutants were identified as being defective in Fe(II) oxidation: eight mutants had general photosynthetic growth defects, and the other six were specifically defective in Fe(II) oxidation. BLAST analysis performed on DNA sequences flanking the mariner insertions revealed that the sequence flanking the transposon has significant similarity to sequences from the genome of *R. palustris* strain CGA009 (38) in all cases.

The eight mutants exhibiting general growth defects grew at least 50% less on acetate or H_2 compared to the wild type (data not shown). Two of these mutants were disrupted in genes that are homologs of *bchZ* and *bchX*, known to encode proteins involved in bacteriochlorophyll synthesis (8). It is not surprising that our screen picked up components of the general photosynthetic electron transport system, given the large variance in cell density in the step prior to the cell suspension assay. Two mutants, however, were identified that are specifically defective in Fe(II) oxidation: 76H3 and A2. 76H3 is a representative of five mutants that have transposon insertions at different locations in the same gene, whereas A2 was only isolated once. Both mutants exhibit normal photosynthetic growth in minimal medium with H_2 as the electron donor, but their ability to oxidize Fe(II) is less than 10% of the wild type (Fig. 7A and B). Complementation of the disrupted genes indicates that their expression is necessary and sufficient to restore nearly wild-type levels of activity, suggesting that Fe(II) oxidation defects are not caused by the downstream genes (Fig. 7C and D).

Because the sequence fragments from TIE-1 flanking the transposon insertions were highly similar to sequences from strain CGA009, we designed primers based on the CGA009 genome to sequence the regions surrounding the transposon insertions in 76H3 and A2 (Fig. 7D). Both regions contained homologs of genes found in the same order in CGA009. Mutant 76H3 has a transposon insertion in a gene that shares 99% identity over the entire gene sequence (791 bp) to gene RPA0198 in *R. palustris* CGA009, which encodes a putative integral membrane protein. The BLAST search predicts that the protein encoded by this gene shares 100% identity to a possible transport protein in *R. palustris* CGA009, 85% identity to a probable ABC transport permease in *Bradyrhizobium japonicum*, and 60% identity to a hypothetical transmembrane protein from *Magnetospirillum* sp. strain MS-1. It is predicted to encode a cytoplasmic membrane protein with six internal helices, based on sequence analysis with the Psort program (http://www.psort.org/). No known motifs could be identified in this protein by the MotifScan program (http://myhits.isb-sib.ch/cgi-bin/motif_scan). Based on the annotation of the CGA009 genome, the upstream genes encode a putative ABC transporter permease (RPA0197) and a putative ABC transporter ATP-binding protein (RPA0196). The downstream gene (RPA0199) encodes a putative phosphinothricin acetyltransferase.

Mutant A2 has a transposon insertion in a gene that shares 99% identity over the entire gene sequence (995 bp) to gene RPA0498 in *R. palustris* CGA009, which is annotated as a *cobS* gene. The translated protein sequence is 100% identical to a putative CobS in strain CGA009, 93% identical to a putative CobS from *Bradyrhizobium japonicum*, 80% identical to a well-studied CobS from *Pseudomonas denitrificans*, and 76% and 71% identical to MoxR-like ATPases from *Rhodospirillum rubrum* and *Rhodobacter sphaeroides*, respectively. Studies of CobS function in *P. denitrificans* have shown that CobS is a cobaltochelatase—a cytoplasmic protein involved in cobalt insertion into porphyrin rings (16). MoxR-like ATPases belong to the AAA superfamily of proteins with *a*ssociated *A*TPase *a*ctivity (30). Not surprisingly, members of the MoxR family function as chaperones/chelatases in the assembly of specific metal-containing enzymatic complexes. Based on the annotation of the CGA009 genome, the genes downstream appear to encode an *N*-acetylglutamate synthase and related acetyltransferases (RPA0497), a CobT homolog (RPA0496), and a conserved hypothetical protein (RPA0495).

DISCUSSION

We have isolated and characterized a genetically tractable Fe(II)-oxidizing bacterium, *Rhodopseudomonas palustris* strain TIE-1. Two Fe(II)-oxidizing strains of *R. palustris* have been reported previously (20, 28, 57). Based strictly on morphological characteristics, an Fe(II)-oxidizing *R. palustris*-like strain was first isolated from an iron-rich ditch in Germany (20). This isolate did not oxidize iron completely and ceased to grow at a grayish green intermediate oxidation state; it was not maintained in culture collections (F. Widdel, personal communication). Although the type strain *R. palustris* DSM123^T was found to be incapable of Fe(II) oxidation by Ehrenreich and Widdel (20), Heising and Schink (28) claimed it was capable of Fe(II) oxidation (28). In this study, we tested the Fe(II) oxidation capacity of the *R. palustris* CGA009 strain, whose genome has been sequenced. Strain CGA009 is not able to grow photoautotrophically on H_2 or Fe(II); however, photoheterotrophically grown cells (using acetate as the electron donor) can slowly oxidize Fe(II) in the cell suspension assay at a similar rate to

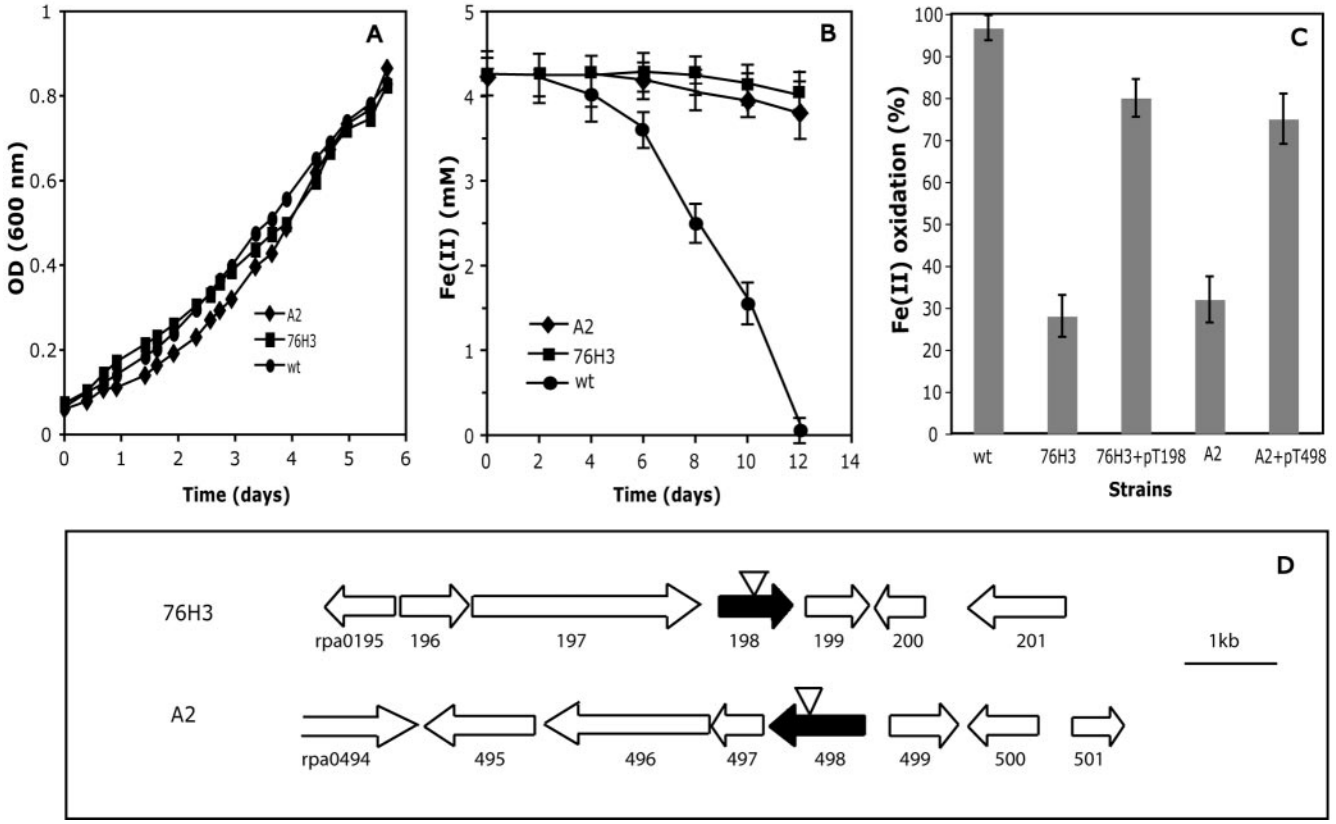

FIG. 7. Mutants 76H3 and A2 are specifically defective in Fe(II) oxidation. (A) Normal growth of mutants 76H3 and A2 with H_2 as the electron donor. Data are representative of two independent cultures. (B) Defects in phototrophic Fe(II) oxidation for mutants 76H3 and A2 compared to wild type. Growth was stimulated with H_2 present in the headspace initially. Data are representative of duplicate cultures. (C) Mutants 76H3 and A2 carrying plasmids pT198 and pT498, respectively, show 80% Fe(II) oxidation compared to the wild type in the cell suspension assay. (D) Organization of the genomic regions surrounding the mutated genes in mutants 76H3 and A2. The black arrows indicate the disrupted genes, and the transposon insertion sites are marked by the open triangles. The numbers provided below the open reading frames (all arrows) are consistent with the numbers given for the identical regions from the CGA009 genome.

that achieved by acetate-grown cell suspensions of strain TIE-1 (unpublished data). In contrast, strain TIE-1 can grow photoautotrophically with H_2 and Fe(II), and H_2-grown cell suspensions readily oxidize Fe(II) at rates much higher than those achieved by acetate-grown cell suspensions.

Rates and products of phototrophic Fe(II) oxidation by TIE-1 are pH dependent. The amount of Fe(II) oxidation is significantly less at pHs higher than 7.0, compared to that oxidized at optimal pH, but this is not due to a growth defect. Previous interpretations of a similar result by Heising and Schink suggested that this might be due to the lower solubility of Fe(II) at higher pH (28). Although our measurements indicate that the total amount of dissolved Fe(II) in our system does not appreciably decrease as pH increases, more subtle species dynamics may control the bioavailability of Fe(II) under these conditions. The transformation from poorly crystalline ferric (hydr)oxides to more crystalline ferric (hydr)oxides is promoted by the adsorption of Fe(II) species onto the solid phase (61). Given that the point of zero charge for ferric (hydr)oxide likely occurs at the upper end of our pH spectrum (3), we would expect cationic Fe(II) species to adsorb to the ferric (hydr)oxides as the point of zero charge is reached and then exceeded with increasing pH. Interestingly, the abiotic oxidation rate of $Fe(OH)^+$ in both freshwater and seawater has been found to be 10^7 times greater than that of Fe^{2+} (45). Moreover, $Fe(OH)_{2(aq)}$ is thought to be the most readily oxidized form of Fe(II) over a pH range of 6 to 8 and the rate-limiting step for the oxidation of Fe^{2+} under these conditions (45). Assuming $Fe(OH)_{2(aq)}$ or $Fe(OH)^+$ is the preferred species taken up or bound by TIE-1, the decrease in Fe(II) oxidation measured coincident with magnetite formation in our medium could be explained if sorption of these species by ferric (hydr)oxides out-competed their sorption/uptake by the cell. Alternatively, it is possible that the decrease in Fe(II) oxidation is due to the inactivation of a biomolecule involved in Fe(II) binding, uptake, and/or oxidation at high pH.

Independent of whether magnetite formation affects the bioavailability of Fe(II), it is noteworthy that magnetite formation can be associated with this type of metabolism. Previous studies with other Fe(II)-oxidizing phototrophs only found various forms of ferric oxides (e.g., goethite and lepidocrocite) to accumulate in the culture medium over time; magnetite was never observed (14, 31, 52). In contrast, magnetite formation following an intermediate state of green rust was reported for the nitrate-dependent Fe(II)-oxidizing bacterium *Dechlorosoma suillum* strain PS (9). Magnetite formation has been

reported for dissimilatory iron-reducing bacteria (DIRB), with magnetite formed through the reduction of ferric oxide (39). Magnetite formation by TIE-1 is unlikely to be formed through the re-reduction of Fe(III), however, based on the evidence that TIE-1 is unable to reduce Fe(III) citrate with acetate as the electron donor in the dark. Considering the differences in the chemistry of the medium used to grow these bacteria, the simplest way to account for magnetite formation in some, but not all, of these cases is that differences in medium chemistry controlled the amount and speed of Fe(II) adsorption onto ferric (hydr)oxides (61). Because pH 7.5 is a reasonable pH value for ancient seawater (25), it is possible that the primary magnetite found in BIFs may record the activity of Fe(II)-oxidizing phototrophs. However, this interpretation does not exclude the possibility that magnetite in BIFs may also have been facilitated by DIRB or abiotic processes (48).

To begin to identify genes involved in phototrophic Fe(II) oxidation, we first needed to develop an efficient method for generating random chromosomal insertions in TIE-1. Transposon mutagenesis has been shown to work in the *Rhodospirillaceae* family, but with mixed success (18). For example, transposition by Tn*5* derivatives was found to transpose in *R. capsulatus* and *R. rubrum* with frequencies of 10^{-4} to 10^{-5} (24, 33); however, for *R. palustris* strain CGA009 and strain EPT100, Tn*5* derivatives were either not successful or very inefficient (21). The fact that the hyperactive mariner transposon used in this study transposes randomly and at high frequencies in TIE-1 suggests that this type of transposon may be an effective mutagenic tool for other *R. palustris* strains.

Out of a total of 12,000 mutants screened for their ability to oxidize Fe(II) in the cell suspension assay, only 6 were identified as being specifically defective in Fe(II) oxidation and only 2 genes were implicated in this process. It is intriguing that both of these genes are also present in *R. palustris* strain CGA009, although this organism cannot grow on Fe(II). Given that photoheterotrophically grown cells of CGA009 can oxidize Fe(II) in the cell suspension assay comparably to TIE-1 when grown under the same conditions, this indicates that Fe(II) oxidation can be decoupled from growth. However, our cell suspension assay did not decouple Fe(II) oxidation from the photosynthetic apparatus, as no Fe(II) oxidation occurred in the dark. It will be interesting to learn what allows TIE-1 but not CGA009 to conserve energy from Fe(II) oxidation for growth. It is possible that essential genes for this process are missing from CGA009, mutated, or not expressed. To resolve this, a screen could be performed to identify TIE-1 mutants that are incapable of phototrophic growth on Fe(II), or CGA009 could be complemented for growth on Fe(II) through provision of genes from TIE-1 (13).

Although much remains to be learned about how TIE-1 oxidizes and grows on Fe(II), the two mutants identified in this study provide important new information. Strain A2 contains a disruption in a homolog of a cobalt chelatase (CobS). Because the structures of cobaltochelatases and ferrochelatases [which insert Fe(II) into porphyrin rings] are similar, it has been suggested that they have similar enzymatic activities (15, 50). While it is possible that the phenotype of A2 might be due to the disruption of an enzyme that inserts Fe(II) into a protein or a cofactor that is involved in Fe(II) oxidation, this seems unlikely, because cobatochelatases and ferrochelatases are typically different at the amino acid level (15). We hypothesize, instead, that a protein involved in Fe(II) oxidation requires cobalamin as cofactor indirectly. In contrast, strain 76H3 is disrupted in a gene that appears to encode a component of an ABC transport system that is located in the cytoplasmic membrane. While a variety of things could be transported by this system, whatever is being transported [e.g., the Fe(II) oxidase or a protein required for its assembly] likely resides at least momentarily in the periplasm. This raises the question of where Fe(II) is oxidized in the cell. Because Fe(II) is known to enter the periplasmic space of gram-negative bacteria through porins in the outer membrane, it is conceivable that Fe(II) could be oxidized in this compartment; alternatively, the Fe(II) oxidase could reside in the outer membrane and face the external environment, as has been inferred for Fe(II)-oxidizing acidophilic bacteria (23, 59). Determining what catalyzes Fe(II) oxidation and where it is localized are the most important next steps in our investigation of the molecular basis of phototrophic Fe(II) oxidation. The isolation of the genetically tractable strain TIE-1 will enable these studies.

ACKNOWLEDGMENTS

We are indebted to Randall E. Mielke for TEM imaging and Elizabeth A. Ottesen for help in constructing the 16S phylogenetic tree. We thank Arash Komeili and Jeff Gralnick for guidance throughout this study and all the Newman lab members for helpful discussions.

This work was supported by a grant from the Packard Foundation to D.K.N. and a postdoctoral fellowship from the German Research Foundation to A.K.

REFERENCES

1. **Appia-Ayme, C., A. Bengrine, C. Cavazza, M. T. Giudici-Orticoni, M. Ruschi, M. Chippaux, and V. Bonnefoy.** 1998. Characterization and expression of the co-transcribed *cyc1* and *cyc2* genes encoding the cytochrome c_4 (c_{552}) and a high-molecular-mass cytochrome c from *Thiobacillus ferrooxidans* ATCC33020. FEMS Microbiol. Lett. **167:**171–177.
2. **Appia-Ayme, C., N. Guiliani, J. Ratouchniak, and V. Bonnefoy.** 1999. Characterization of an operon encoding two *c*-type cytochromes, an aa_3-type cytochrome oxidase, and rusticyanin in *Thiobacillus ferrooxidans* ATCC 33020. Appl. Environ. Microbiol. **65:**4781–4787.
3. **Baltpurvins, K. A., R. C. Burns, G. A. Lawrance, and A. D. Stuart.** 1997. Effect of Ca^{2+}, Mg^{2+}, and anion type on the aging of iron(III) hydroxide precipitates. Environ. Sci. Technol. **31:**1024–1032.
4. **Benz, M., A. Brune, and B. Schink.** 1998. Anaerobic and aerobic oxidation of ferrous iron at neutral pH by chemoheterotrophic nitrate-reducing bacteria. Arch. Microbiol. **169:**159–165.
5. **Blake, R. C., E. A. Shute, J. Waskovsky, and A. P. J. Harrison.** 1992. Respiratory components in acidophilic bacteria that respire iron. Geomicrobiol. J. **10:**173–192.
6. **Bradford, M. M.** 1976. Rapid and sensitive method for quantitation of microgram quantities of protein utilizing principle of protein-dye binding. Anal. Biochem. **72:**248–254.
7. **Britton, G.** 1995. Structure and properties of carotenoids in relation to function. FASEB J. **9:**1551–1558.
8. **Burke, D. H., M. Alberti, and J. E. Hearst.** 1993. The *Rhodobacter capsulatus* chlorin reductase-encoding locus, *bchA*, consists of three genes, *bchX*, *bchY*, and *bchZ*. J. Bacteriol. **175:**2407–2413.
9. **Chaudhuri, S. K., J. G. Lack, and J. D. Coates.** 2001. Biogenic magnetite formation through anaerobic biooxidation of Fe(II). Appl. Environ. Microbiol. **67:**2844–2848.
10. **Chiang, S. L., and E. J. Rubin.** 2002. Construction of a mariner-based transposon for epitope-tagging and genomic targeting. Gene **296:**179–185.
11. **Cobley, J. G., and B. A. Haddock.** 1975. Respiratory chain of *Thiobacillus ferrooxidans*—reduction of cytochromes by Fe^{2+} and preliminary characterization of rusticyanin, a novel blue copper protein. FEBS Lett. **60:**29–33.
12. **Cox, J. C., and D. H. Boxer.** 1978. Purification and some properties of rusticyanin, a blue copper protein involved in iron(II) oxidation from *Thiobacillus ferrooxidans*. Biochem. J. **174:**497–502.
13. **Croal, L. R., J. A. Gralnick, D. Malasarn, and D. K. Newman.** 2004. The genetics of geochemistry. Annu. Rev. Genet. **38:**175–202.
14. **Croal, L. R., C. M. Johnson, B. L. Beard, and D. K. Newman.** 2004. Iron isotope fractionation by Fe(II)-oxidizing photoautotrophic bacteria. Geochim. Cosmochim. Acta **68:**1227–1242.

15. **Dailey, H. A., T. A. Dailey, C. K. Wu, A. E. Medlock, K. F. Wang, J. P. Rose, and B. C. Wang.** 2000. Ferrochelatase at the millennium: structures, mechanisms and 2Fe-2S clusters. Cell. Mol. Life Sci. **57:**1909–1926.
16. **Debussche, L., M. Couder, D. Thibaut, B. Cameron, J. Crouzet, and F. Blanche.** 1992. Assay, purification, and characterization of cobaltochelatase, a unique complex enzyme catalyzing cobalt insertion in hydrogenobyrinic acid *a,c*-diamide during coenzyme B_{12} biosynthesis in *Pseudomonas denitrificans*. J. Bacteriol. **174:**7445–7451.
17. **Dehio, C., and M. Meyer.** 1997. Maintenance of broad-host-range incompatibility group P and group Q plasmids and transposition of Tn*5* in *Bartonella henselae* following conjugal plasmid transfer from *Escherichia coli*. J. Bacteriol. **179:**538–540.
18. **Donohue, T. J., and S. Kaplan.** 1991. Genetic techniques in *Rhodospirillaceae*. Methods Enzymol. **204:**459–485.
19. **Edwards, K. J., P. L. Bond, T. M. Gihring, and J. F. Banfield.** 2000. An archaeal iron-oxidizing extreme acidophile important in acid mine drainage. Science **287:**1796–1799.
20. **Ehrenreich, A., and F. Widdel.** 1994. Anaerobic oxidation of ferrous iron by purple bacteria, a new-type of phototrophic metabolism. Appl. Environ. Microbiol. **60:**4517–4526.
21. **Elder, D. J. E., P. Morgan, and D. J. Kelly.** 1993. Transposon Tn*5* mutagenesis in *Rhodopseudomonas palustris*. FEMS Microbiol. Lett. **111:**23–30.
22. **Emerson, D., and C. Moyer.** 1997. Isolation and characterization of novel iron-oxidizing bacteria that grow at circumneutral pH. Appl. Environ. Microbiol. **63:**4784–4792.
23. **Fukumori, Y., T. Yano, A. Sato, and T. Yamanaka.** 1988. Fe(II)-oxidizing enzyme purified from *Thiobacillus ferrooxidans*. FEMS Microbiol. Lett. **50:** 169–172.
24. **Ghosh, R., D. J. E. Elder, R. Saegesser, D. J. Kelly, and R. Bachofen.** 1994. An improved procedure and new vectors for transposon Tn*5* mutagenesis of the phototrophic bacterium *Rhodospirillum rubrum*. Gene **150:**97–100.
25. **Grotzinger, J. P., and J. F. Kasting.** 1993. New constraints on precambrian ocean composition. J. Geol. **101:**235–243.
26. **Hawley, R. S., and M. Y. Walker.** 2003. Advanced genetic analysis. Blackwell Science Ltd., Malden, Mass.
27. **Heising, S., L. Richter, W. Ludwig, and B. Schink.** 1999. *Chlorobium ferrooxidans* sp. nov., a phototrophic green sulfur bacterium that oxidizes ferrous iron in coculture with a "*Geospirillum*" sp. strain. Arch. Microbiol. **172:**116–124.
28. **Heising, S., and B. Schink.** 1998. Phototrophic oxidation of ferrous iron by a *Rhodomicrobium vannielii* strain. Microbiol. UK **144:**2263–2269.
29. **Ingledew, W. J., and J. G. Cobley.** 1980. A potentiometric and kinetic study on the respiratory chain of ferrous-iron-grown *Thiobacillus ferrooxidans*. Biochim. Biophys. Acta **590:**141–158.
30. **Iyer, L. M., D. D. Leipe, E. V. Koonin, and L. Aravind.** 2004. Evolutionary history and higher order classification of AAA plus ATPases. J. Struct. Biol. **146:**11–31.
31. **Kappler, A., and D. K. Newman.** 2004. Formation of Fe(III) minerals by Fe(II)-oxidizing photoautotrophic bacteria. Geochim. Cosmochim. Acta **68:** 1217–1226.
32. **Keen, N. T., S. Tamaki, D. Kobayashi, and D. Trollinger.** 1988. Improved broad-host-range plasmids for DNA cloning in gram-negative bacteria. Gene **70:**191–197.
33. **Kelly, D. J., D. J. Richardson, S. J. Ferguson, and J. B. Jackson.** 1988. Isolation of transposon Tn5 insertion mutants of *Rhodobacter capsulatus* unable to reduce trimethylamine-N-oxide and dimethylsulfoxide. Arch. Microbiol. **150:**138–144.
34. **Kim, M. K., and C. S. Harwood.** 1991. Regulation of benzoate-CoA ligase in *Rhodopseudomonas palustris*. FEMS Microbiol. Lett. **83:**199–203.
35. **Kompantseva, E. I., E. E. Panteleeva, E. V. Ariskina, A. M. Lysenko, J. F. Imhoff, and V. M. Gorlenko.** 1996. Phylogenetic relationships among budding purple bacteria of the genus Rhodopseudomonas. Microbiology **65:** 344–351.
36. **Konhauser, K. O., T. Hamade, R. Raiswell, R. C. Morris, F. G. Ferris, G. Southam, and D. E. Canfield.** 2002. Could bacteria have formed the precambrian banded iron formations? Geology **30:**1079–1082.
37. **Lack, J. G., S. K. Chaudhuri, R. Chakraborty, L. A. Achenbach, and J. D. Coates.** 2002. Anaerobic biooxidation of Fe(II) by *Dechlorosoma suillum*. Microb. Ecol. **43:**424–431.
38. **Larimer, F. W., P. Chain, L. Hauser, J. Lamerdin, S. Malfatti, L. Do, M. L. Land, D. A. Pelletier, J. T. Beatty, A. S. Lang, F. R. Tabita, J. L. Gibson, T. E. Hanson, C. Bobst, J. Torres, C. Peres, F. H. Harrison, J. Gibson, and C. S. Harwood.** 2004. Complete genome sequence of the metabolically versatile photosynthetic bacterium *Rhodopseudomonas palustris*. Nat. Biotechnol. **22:** 55–61.
39. **Lovley, D. R., J. F. Stolz, G. L. Nord, and E. J. P. Phillips.** 1987. Anaerobic production of magnetite by a dissimilatory iron- reducing microorganism. Nature **330:**252–254.
40. **Ludwig, W., O. Strunk, R. Westram, L. Richter, H. Meier, Yadhukumar, A. Buchner, T. Lai, S. Steppi, G. Jobb, W. Forster, I. Brettske, S. Gerber, A. W. Ginhart, O. Gross, S. Grumann, S. Hermann, R. Jost, A. Konig, T. Liss, R. Lussmann, M. May, B. Nonhoff, B. Reichel, R. Strehlow, A. Stamatakis, N. Stuckmann, A. Vilbig, M. Lenke, T. Ludwig, A. Bode, and K. H. Schleifer.** 2004. ARB: a software environment for sequence data. Nucleic Acids Res. **32:**1363–1371.
41. **Madigan, M. T., J. M. Martinko, and J. Parker.** 2002. Brock biology of microorganisms, 10th ed., p. A-4. Prentice Hall, Upper Saddle River, N.J.
42. **Mansch, R., and W. Sand.** 1992. Acid-stable cytochromes in ferrous iron oxidizing cell-free preparations from *Thiobacillus ferrooxidans*. FEMS Microbiol. Lett. **92:**83–88.
43. **Mehrabi, S., U. M. Ekanemesang, F. O. Aikhionbare, K. S. Kimbro, and J. Bender.** 2001. Identification and characterization of *Rhodopseudomonas* spp., a purple, non-sulfur bacterium from microbial mats. Biomol. Engin. **18:**49–56.
44. **Miller, J. H.** 1992. A short course in bacterial genetics. Cold Spring Harbor Laboratory Press, Cold Spring Harbor, N.Y.
45. **Millero, F. J.** 1985. The effect of ionic interactions on the oxidation of metals in natural waters. Geochim. Cosmochim. Acta **49:**547–553.
46. **Mjoji, N., and C. F. Kulpa.** 1988. Identification of a unique outer membrane protein required for Fe(II) oxidation in *Thiobacillus ferrooxidans*, p. 89–102. *In* P. R. Norris and D. P. Kelly (ed.), Biohydrometallurgy. STL, Kew Surrey, United Kingdom.
47. **Morel, F., and J. G. Hering.** 1993. Principles and applications of aquatic chemistry. Wiley-Interscience, New York, N.Y.
48. **Morris, R. C.** 1993. Genetic modeling for banded iron-formation of the Hamersley group, Pilbara craton, Western Australia. Precambrian Res. **60:** 243–286.
49. **Raponi, M., I. W. Dawes, and G. M. Arndt.** 2000. Characterization of flanking sequences using long inverse PCR. BioTechniques **28:**838–842.
50. **Roth, J. R., J. G. Lawrence, and T. A. Bobik.** 1996. Cobalamin (coenzyme B-12): synthesis and biological significance. Annu. Rev. Microbiol. **50:**137–181.
51. **Stookey, L. L.** 1970. Ferrozine—a new spectrophotometric reagent for iron. Anal. Chem. **42:**779–781.
52. **Straub, K. L., M. Benz, and B. Schink.** 2001. Iron metabolism in anoxic environments at near neutral pH. FEMS Microbiol. Ecol. **34:**181–186.
53. **Straub, K. L., F. A. Rainey, and F. Widdel.** 1999. *Rhodovulum iodosum* sp. nov. and *Rhodovulum robiginosum* sp. nov., two new marine phototrophic ferrous-iron-oxidizing purple bacteria. Int. J. Syst. Bacteriol. **49:**729–735.
54. **Suter, D., C. Siffert, B. Sulzberger, and W. Stumm.** 1988. Catalytic dissolution of iron(III) (hydr)oxides by oxalic acid in the presence of Fe(II). Naturwissenschaften **75:**571–573.
55. **Temple, K. L., and A. R. Colmer.** 1951. The autotrophic oxidation of iron by a new bacterium, *Thiobacillus ferrooxidans*. J. Bacteriol. **62:**605–611.
56. **Valkova-Valchanova, M. B., and S. H. P. Chan.** 1994. Purification and characterization of 2 new c-type cytochromes involved in Fe^{2+} oxidation from *Thiobacillus ferrooxidans*. FEMS Microbiol. Lett. **121:**61–69.
57. **Widdel, F., S. Schnell, S. Heising, A. Ehrenreich, B. Assmus, and B. Schink.** 1993. Ferrous iron oxidation by anoxygenic phototrophic bacteria. Nature **362:**834–836.
58. **Yamanaka, T., and Y. Fukumori.** 1995. Molecular aspects of the electron transfer system which participates in the oxidation of ferrous ion by *Thiobacillus ferrooxidans*. FEMS Microbiol. Rev. **17:**401–413.
59. **Yamanaka, T., T. Yano, M. Kai, H. Tamegai, A. Sato, and Y. Fukumori.** 1991. The electron transfer system in an acidophilic iron-oxidizing bacterium, p. 223–246. *In* Y. Mukohata (ed.), New era of bioenergetics. Academic Press, Tokyo, Japan.
60. **Yarzabal, A., G. Brasseur, and V. Bonnefoy.** 2002. Cytochromes c of *Acidithiobacillus ferrooxidans*. FEMS Microbiol. Lett. **209:**189–195.
61. **Zachara, J. M., R. K. Kukkadapu, J. K. Fredrickson, Y. A. Gorby, and S. C. Smith.** 2002. Biomineralization of poorly crystalline Fe(III) oxides by dissimilatory metal reducing bacteria (DMRB). Geomicrobiol. J. **19:**179–207.